

Supplementary materials for: Far-field Unlabeled Super Resolution Imaging with Superoscillatory Illumination

Edward T. F. Rogers^{1,2*}, Shmma Quraishie³, Katrine S. Rogers⁴, Tracey A. Newman³, Peter J. S. Smith^{1,5,6}, and Nikolay I. Zheludev^{2,7}

¹*Institute for Life Sciences, University of Southampton, Highfield, Southampton SO17 1BJ, UK*

²*Optoelectronics Research Centre and Centre for Photonic Metamaterials, University of Southampton, Highfield, Southampton SO17 1BJ, UK*

³*Clinical and Experimental Sciences, Faculty of Medicine, University of Southampton, Southampton, SO17 1BJ, UK*

⁴*School of Mathematics and Statistics, The Open University, Walton Hall, Milton Keynes, MK7 6AA, UK*

⁵*Biological Sciences, Faculty of Natural and Environmental Sciences, University of Southampton, Southampton, SO17 1BJ, UK*

⁶*Marine Biological Laboratory, Woods Hole, MA 02543, USA*

⁷*Centre for Disruptive Photonic Technologies, The Photonic Institute, School of Physical and Mathematical Sciences, Nanyang Technological University, 637371, Singapore*

*E.T.F.Rogers@soton.ac.uk

Construction of the microscope

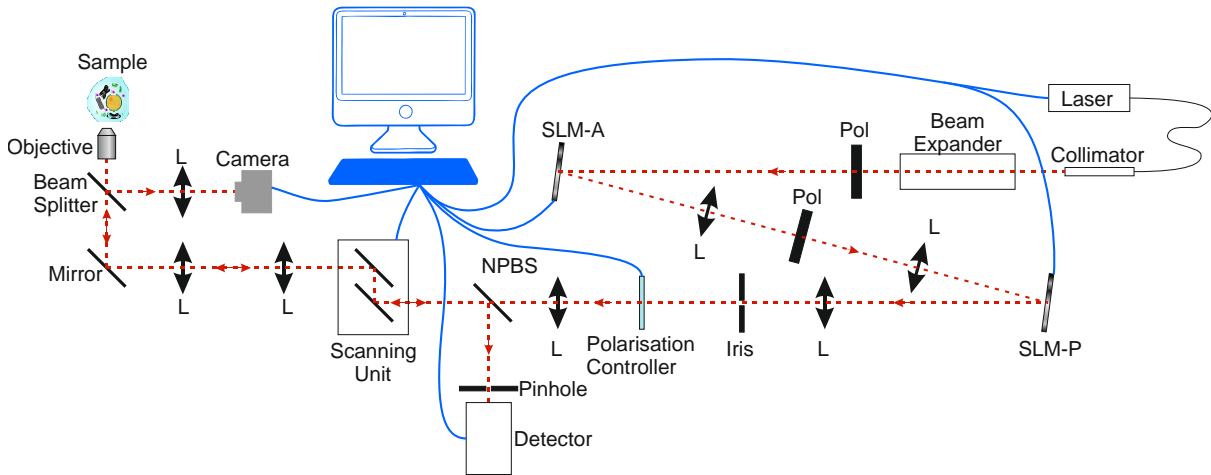


Figure 1S: **Schematic of the superoscillatory microscope.** Pol – Polariser, SLM-A – Spatial light modulator used in amplitude modulation mode, L – Lens, SLM-P – Spatial light modulator used in phase modulation mode, NPBS – Non-polarising beam splitter.

An optical schematic of our superoscillatory microscope is shown in Figure 1S. The superoscillatory microscope system is built on the basis of a confocal Nikon Ti-E microscope stand with a 100X, 1.4 NA objective (Nikon MRD01901) and a resonant-galvo scanning

system capable of 30 frames per second (fps) capture. Although we used an objective with NA=1.4, to reduce the aberrations in the formation of the superoscillatory spots, we restricted the illuminating NA to 1.0 by restricting the diameter of the beam illuminating the lens. Effective pixel size on the scanned image was typically 20nm x 20nm. For live cell imaging, we used a temperature-controlled enclosure (Solent Scientific) operating at 37°C. The microscope was modified by adding two spatial light modulators (Meadowlark P512), and a laser source (Newport Excelsior-ONE 488nm, 100mW) for illumination. Raw images were captured at 30 fps and then averaged over 9 frames to achieve a non-polarised image at 3.3 fps. When polarisation contrast mode was used, 4 frames were required to build each image in the video sequence. This reduced the framerate to 0.83 frames per second. The input laser power as measured at the input to the microscope scanning unit was ~100 μ W. To filter out the halo in superoscillatory images, we use a 35 μ m (0.77 Airy units) pinhole in front of the detector.

To control the polarisation state of the light incident on our sample in polarisation contrast mode, we used a polarisation controller¹ (The OpenPolScope Resource, Woods Hole, Mass, USA). We calculated the magnitude of anisotropy, D , and polarisation azimuth, φ , using²:

$$D = 2 \frac{\sqrt{(I_0 - I_{90})^2 + (I_{45} - I_{135})^2}}{I_0 + I_{45} + I_{90} + I_{135}}$$

$$\varphi = \frac{1}{2} \tan^{-1} \left(\frac{I_{45} - I_{135}}{I_0 - I_{90}} \right).$$

To account for polarisation distortions in the microscope optics, we performed in-situ polarisation calibrations using reflective nanogratings. Slow gradient distortions in the captured images were corrected by reference to empty (control) parts of the sample. In some cases, to enhance visibility of the polarisation contrast, the brightness histograms were slightly stretched such that 0.1% of the dimmest and brightest pixels appeared saturated. Unmodified images are available in the dataset for this paper.

Comparison with confocal imaging

For a clear comparison of the resolving power of our instrument against conventional techniques, we have simulated imaging of the both the Siemens star sample from the main text and a test sample consisting of pairs of holes in an opaque film. We compare brightfield imaging of the test sample with conventional confocal and superoscillatory scanning-mode images using the same microscope and objective lens. The simulations show significantly enhanced resolution of the Siemens star between confocal and superoscillatory modes – lines are visible closer to the centre. In the hole sample, at the operational wavelength of 488nm, brightfield imaging can merely resolve holes separated by 350nm. While confocal has a resolution improvement over brightfield, the superoscillatory instrument is clearly better still, and can resolve holes separated by 200nm. This trend is also seen in recently published experimental data³. This closely matches both the resolution seen in the experimental Siemens star images (see main text) and the superoscillatory hotspot size.

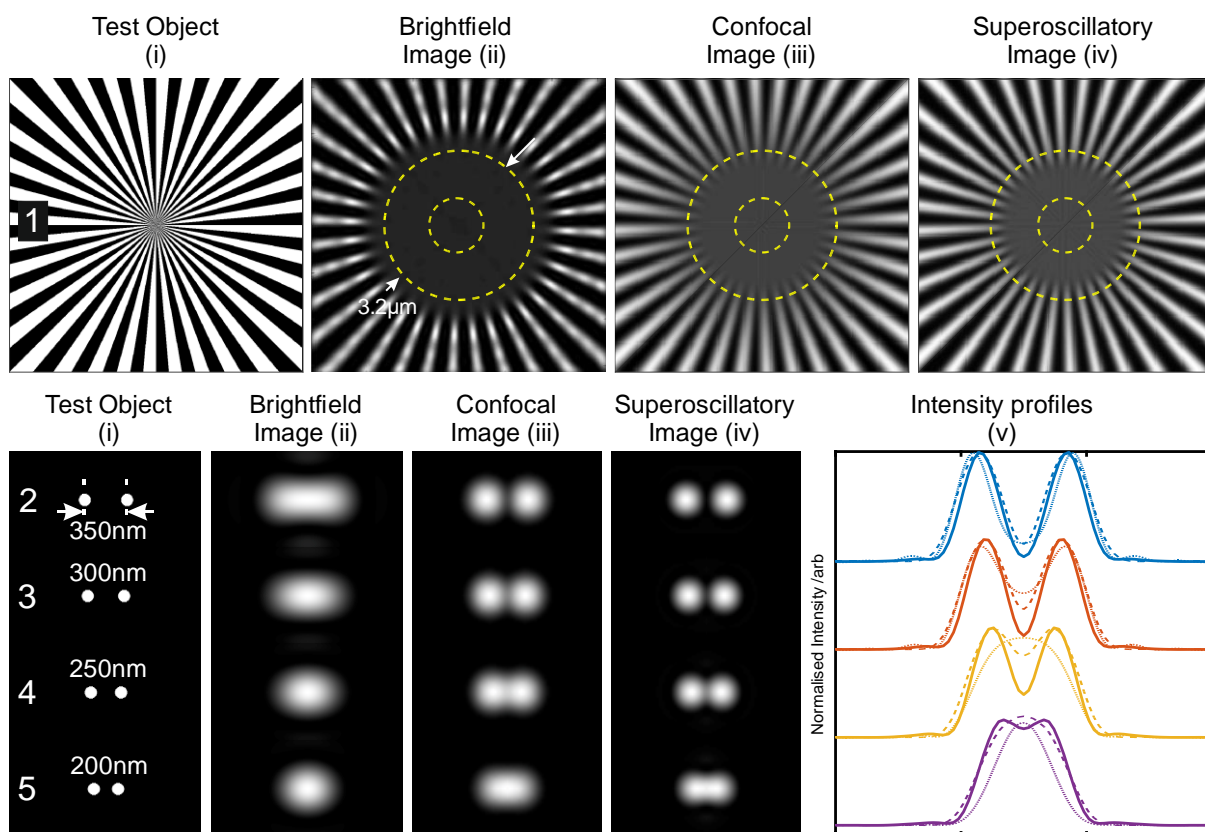


Figure 2S: **Resolution improvement in a superoscillatory microscope.** Simulations of imaging a Siemens star sample and pairs of holes in opaque screen. Columns show: (i) test sample design (Siemens star (row 1) or pairs of 50nm holes in a reflecting screen spaced by different distances from 350nm to 200nm (rows 2-5)) ; Columns (ii, iii and iv) show images taken (ii) in bright field regime with conventional lens; (iii) confocal imaging with standard illumination and (iv) with superoscillatory illumination. Column (v) shows intensity (vertically integrated) over the hole images, (dotted: bright field; dashed: confocal; solid: superoscillatory) showing the resolution achieved. At the wavelength of 488nm brightfield imaging with a conventional lens only resolves holes separated by 350nm, while holes separated by only 200nm can be resolved with superoscillatory illumination.

Captions for supplementary videos

These videos correspond to the still images in Figure 7 of the main text and show the range of cell morphologies to which our technique can be successfully applied. The MG63 cells are thick, with significant internal structuring, compared to the thin neuronal process. In video 1 and 3, filopodia are clearly seen extending, moving and retracting, whereas in video 3 retrograde motion from the leading edge of the growth cone towards the neuronal process is hinted at. In all videos, the spatial scale is as given in Figure 4 of the main text.

Supplementary video 1: Polarization-contrast video of an unlabelled MG63 cell. Timelapse imaging at 15 seconds per frame, 5 min duration; played at 3 fps.

Supplementary video 2: Polarization-contrast video of a growth cone in an unlabelled mouse neuron. Timelapse imaging at 10 seconds per frame, 3 min 40 s duration; played at 3 fps.

Supplementary video 3: Non-polarised reflection mode superoscillatory video of an unlabelled MG63 cell. Real-time video captured at 3 fps 1 min 5 s duration; played at 3 fps.

Supplementary video 4: Superoscillatory polarisation-contrast video (magnitude only, green channel) combined with a confocal fluorescently labelled video (MitoTracker red, red channel) of an MG63 cell. Timelapse imaging at 5 seconds per frame, 3 min duration; played at 3 fps.

References

1. Oldenbourg, R. & Mei, G. New polarized light microscope with precision universal compensator. *J. Microsc.* **180**, 140–147 (1995).
2. Mehta, S. B., Shribak, M. & Oldenbourg, R. Polarized light imaging of birefringence and diattenuation at high resolution and high sensitivity. *J. Opt.* **15**, 094007 (2013).
3. Yuan, G., Rogers, K. S., Rogers, E. T. F. & Zheludev, N. I. Far-Field Superoscillatory Metamaterial Superlens. *Phys. Rev. Appl.* **11**, 1 (2019).